lated (as for 47) and subsequently cyclized to optically active 53, examination of the CD curves of all of the products readily demonstrated that no crossover from one enantiomeric series into another had occurred. This unambiguously excludes the cycloreversion process (Scheme IX). To explain the stereochemical outcome of allylation at C-11 (methylation also gives the same stereochemistry, therefore excluding an O-allylation followed by [3.3] sigmatropic rearrangement), we favor the situation where the orbital coefficient at the C-11 anion is high on the endo face because it is trans coplanar to the amide nitrogen lone pair and therefore minimizes the dipole moment along the C-10–C-11 bond in 66. We are current exploring the generality of this phenomenon.

In summary, what started as an extension of our organosilicon research has rapidly developed into a separate program. The ready generation of an indole-2,3-quinodimethane intermediate through imine tautomerism, and its subsequent intramolecular trapping, provides a simple route to *Aspidosperma* alkaloids.

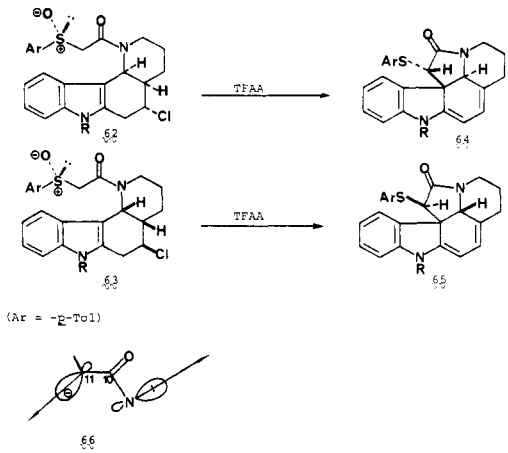

The ability of any strategy to cope with complicated problems and simplify them is the best measure of its value.

The National Institutes of Health are gratefully thanked for their financial support.

Molecular Auger Spectroscopy†

R. R. RYE* and J. E. HOUSTON

Sandia National Laboratories, Albuquerque, New Mexico 87185

Received February 28, 1983 (Revised Manuscript Received August 1, 1983)

Auger electron spectroscopy, despite its widespread application in the area of surface studies,[1] has had only limited application to the study of molecular properties. Even in surface work its application has primarily been in qualitative and quantitative elemental identification. This limited application to molecular studies has largely resulted from the complex nature of the Auger process and the attendant difficulty of extracting detailed electronic information.

The Auger process and the experimental arrangement is illustrated in Figure 1 for the Auger spectroscopy of gas-phase molecules, the topic of this Account. The experimental arrangement involves the intersection of a high-energy (~2 keV) electron beam and a molecular jet diverging into a rapidly pumped chamber. This intersection occurs at the focal point of an electron-energy analyzer, in our case a retarding cylindrical mirror analyzer. The electron beam serves as a convenient way of producing an initial core-state ionization. The experimental arrangement in Figure 1 is limited to samples with vapor pressures $>10^{-3}$ torr, although low vapor pressure samples can be accommodated if necessary by heating the analyzer up to 100 °C. In general, the range of samples open to Auger spectroscopy is the same as that open to X-ray photoelectron spectroscopy. However, for solid samples where electron-beam damage is unacceptable, photon-beam excitation is the preferred mode. For initial core holes in states with less than several kiloelectron volts binding energy, the dominant mode of decay is the Auger process in which the core hole captures a higher lying electron and transfers its excess energy to ejecting a second electron, the Auger electron. As illustrated in Figure 1 for a two-state valence system, the Auger transition involves two electrons and three states,[2] the combination of which can yield three energetically distinct Auger electrons. For first row elements, these transitions are referred to as giving rise to the KVV Auger line. In general, the number of Auger transitions will be greater than the number of possible two-hole valence combinations because of multiplet combinations, and despite the fact that a typical spectrum covers 40–50 eV, one has little hope of resolving individual transitions for any molecule of appreciable size.

Thus, while the Auger process is more complicated than the usual one-electron spectroscopies, e.g., ultra-

Robert Rye was born in Memphis, TN, where he received the B.S. degree from Memphis State University in 1963. After obtaining the Ph.D degree from Iowa State University with R. S. Hansen, he was a member of the Chemistry Department of Cornell University until 1974 when he joined the Surface Science group at Sandia National Laboratories. His basic interests have been in the chemistry of solid surfaces and his current interests in molecular Auger Spectroscopy are directed toward this end.

J. E. Houston received his Ph.D. degree in Physics from the Oklahoma State University in 1965. He joined Sandia National Laboratories after 2 years of teaching in the Physics Department at the South Dakota School of Mines. His research concerns the development and application of various electron spectroscopic techniques for obtaining an understanding of the nature of surfaces and the way in which their properties control the interaction of solids with their environment.

†This work was performed at Sandia National Laboratories and supported by the U.S. Department of Energy under Contract No. DE-AC04-76DP00789.

(1) P. H. Holloway, *Adv. Electron. Electron Phys.*, 54, 241 (1980).
(2) T. A. Carlson, "Photoelectron and Auger Spectroscopy", Plenum Press, New York, 1975.

0001-4842/84/0117-0041$01.50/0

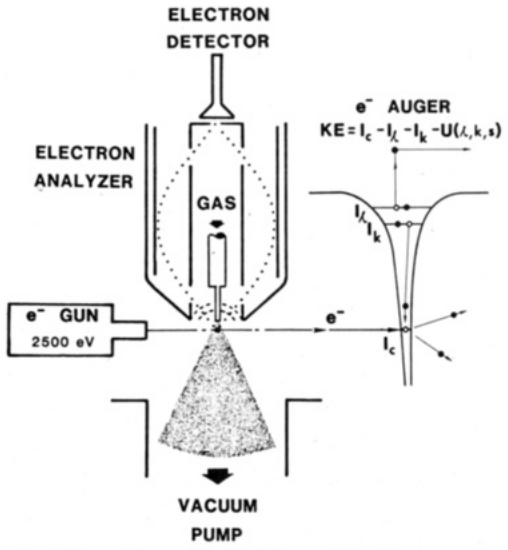

Figure 1. Schematic representation of the Auger process and the apparatus used to obtain gas-phase Auger spectra. Core holes are created at the intersection of the high-energy electron beam and gas jet shown at the left. These coreholes decay by the Auger process depicted at the right for a two-state valence system. The energy distribution of the ejected Auger electrons is obtained by using the electron-energy analyzer and detector, schematically shown at the left. See text for more details.

violet photoelectron spectroscopy, it clearly has unique attributes as a local valence probe, attributes that stem from the direct involvement of the localized core state in the electronic transition. It is the realization of these unique aspects that has lead to the recent increased interest in Auger spectroscopy as a local electronic probe. Although excellent work was done early by Siegbahn et al.[3] and by Moddeman et al.,[4] only recently has suficient data and theoretical understanding become available to permit a systematic study of the information content available from Auger line-shape analysis. Ideally one should analyze Auger spectra in terms of a two-electron theory; however, considerable information can be obtained from an analysis of spectra in terms of a one-lectron description. With this approach, we will show that the information content of an Auger spectrum can be divided into three broad classes.

The most direct level of information is contained in the general "fingerprint" structure of the spectra.[5] From numerous examples, this level of analysis has been shown to be sensitive to the local orbital hybridization with dramatic differences being observed between the sp^3–, sp^2–, and sp-hydridized carbon atoms in the alkanes, alkenes, and alkynes.[6-8] In contrast, similar C(KVV) fingerprint spectra are obtained for such seemingly dissimilar molecules as acetylene and cyanide[8] or ethylene and cyclopropane.[7]

The second level of information contained in the Auger line shape involves the energy of the ejected Auger electron itself. For those cases where a one-electron molecular-orbital description is applicable, the kinetic energy of the ejected electron is given[9,10] by

$$\mathrm{KE} = I_c - I_l - I_k - U(l,k,s) \qquad (1)$$

where the I's refer to core (c) and valence (l, k) one-electron binding energies and the last term is the spin-dependent interaction of the two final-state holes, i.e., their mutual Coulomb repulsion. Equation 1 is an attempt to cast this inherently two-electron process into the more familiar one-electron framework. This works surprisingly well for a number of cases, but one should keep in mind that the complication in the Auger process stems from its two-electron character.

The factor in the energy expression, eq 1, under most intensive theoretical investigation, has been the nature of the Coulomb repulsion term, U.[9-12] For a one-electron-like process, eq 1 would predict an Auger spectrum that is given by a self-fold or convolution of the energy distribution of valence levels in the case of molecules or of the valence band in the case of solids. The value of U, which depends on the separation between the holes, would be essentially zero in the case of solids where the holes are in effect infinitely separated in space but can have an appreciable value in the case of small molecules where a significant Coulomb interaction results from the restricted size. However, it is often found that spectra from solids do not show U values of zero. The classic example of this sort of behavior is solid copper where the spectrum corresponding to the d electrons is found to be atomic like with a nonzero value of U.[13] In this case the final-state holes do not move independently but exhibit highly correlated motion with both holes essentially confined to the same atomic site that contained the initial core hole. Such behavior has been described as being localized. Cini[11] and Sawatzky[12] have shown that the critical parameters that dictate localized behavior in the case of solids is the relative magnitude of U corresponding to localization to a specific site and the bandwidth, W. For $U >> W$ states are split out of the band and localized behavior observed, while for $U << W$ the final states are contained within the band and delocalized or one-electron-like behavior is observed. For diatomic molecules the same basic criterion has been proposed, with W in these cases being given by the splitting between the bonding and antibonding states and U being replaced by ΔU, the difference between U for localized and delocalized holes.[9,10,14] Little theoretical attention has yet been paid to larger molecules, but the approach of Ramaker of dividing the problem into bond, group, and band orbitals[9] appears fruitful.

The involvement of an inherently localized core state in the Auger process leads to a third level of information in which the intensity variation is directly sensitive to the orbital electron density distribution at a given core

(3) K. Siegbahn, C. Nordling, G. Johansson, J. Hodman, P. F. Hodin, K. Hamrin, U. Gelius, T. Bersmark, L. O. Werme, R. Manne, and Y. Baer, "ESCA Applied to Free Molecules", North Holland, Amsterdam, 1969.
(4) W. E. Moddeman, T. A. Carlson, M. O. Krause, B. P. Pullen, W. E. Bull, and G. K. Schweitzer, *J. Chem. Phys.*, **55**, 2317 (1971).
(5) R. R. Rye, T. E. Madey, J. E. Houston, and P. H. Holloway, *J. Chem. Phys.*, **69**, 1504 (1978).
(6) R. R. Rye, D. R. Jennison, and J. E. Houston, *J. Chem. Phys.*, **73**, 4867 (1980).
(7) J. E. Houston and R. R. Rye, *J. Chem. Phys.*, **74**, 71 (1981).
(8) R. R. Rye and J. E. Houston, *J. Chem. Phys.*, **75**, 2085 (1982).
(9) D. E. Ramaker, "International Summer Institute of Surface Science Springer Series in Chemical Physics", Springer-Verlag, New York, in press.
(10) D. R. Jennison, *J. Vac. Sci. Technol.*, *20*, 548 (1982).
(11) M. Cini, *Solid State Commun.*, **20**, 605 (1976); *Surf. Sci.*, **77**, 483 (1979).
(12) G. A. Sawatsky, *Phys. Rev. Lett.*, **39**, 504 (1977); G. A. Sawatsky and A. Lenselink, *Phys. Rev. B*, **21**, 1790 (1980).
(13) E. Antonides, E. C. Janse, and G. A. Sawatsky, *Phys. Rev. B*, **15**, 1669 (1977).
(14) T. D. Thomas and P. Weightman, *Chem. Phys. Lett.*, **B1**, 325 (1981).

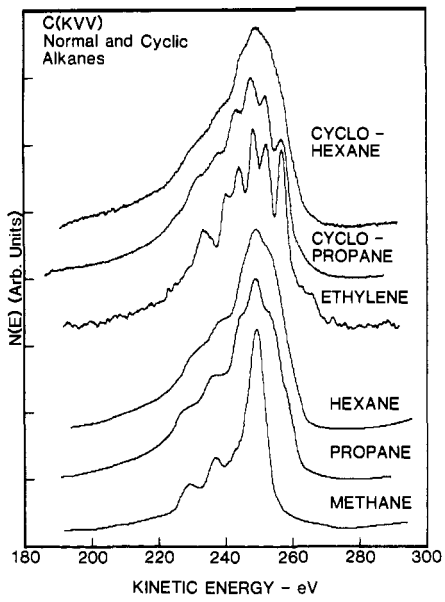

Figure 2. C(KVV) Auger spectra of ethylene and selected normal and cyclic alkanes.

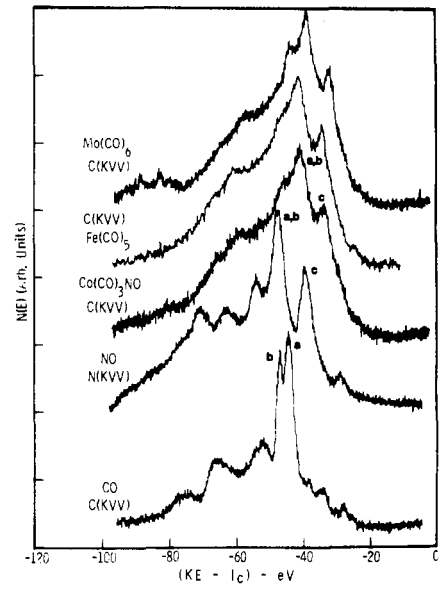

Figure 3. C(KVV) Auger spectra of several metal carbonyls and N(KVV) and C(KVV) spectra of NO and CO plotted on a common two-hole energy scale obtained by subtracting the core binding energies from the respective experimental Auger kinetic energies.

site. The transition rate, or intensity, for the Auger process can be written[9,10] as

$$I = N|\langle\phi_c\phi_f|1/r_{12}|\phi_l\phi_k\rangle|^2 \qquad (2)$$

where N is a statistical factor accounting for the degeneracy of the orbitals involved and the second term is the matrix element connecting the initial core c and continuum f states to the final valence level states l and k. The $1/r_{12}$ term represents the Coulomb interaction. Although l and k in eq 2 refer to molecular orbital states, Matthew and Komninos have shown that the probability is essentially zero for transitions involving valence electron density in the vicinity of an atom other than the one containing the initial core hole.[15] In a LCAO-level approximation this means that one only has to consider the atomic-like terms in the wave function corresponding to the same atom as the core hole. Thus for a core hole on atom A, the intensity for a transition to final-state holes in valence levels l and k can be written as

$$I_A = N[\sum\sum C_{Al}C_{Ak}M_{Alk}]^2 \qquad (3)$$

where the C's are the LCAO mixing coefficients for the atomic orbitals centered on A and M(l,k) is an atomic matrix elment. The Auger transition intensity is, therefore, proportional to the second power of the product of the LCAO coefficients. The atomic matrix element is independent of bonding but dependent on the symmetry properties of the orbitals involved, e.g., whether they are s or p, etc. The same set of valence states, of course, can be accessed from a second core site in the molecule and this may result in different intensities due to the fact that different LCAO coefficients are involved. As a result, a comparison of the Auger intensity pattern as seen from different atomic sites carries information about the spatial extent and electron distribution in the various molecular orbitals.

Local Symmetry Information

Information on the symmetry or hybridization local to an atomic site can be obtained by inspection of the spectral fingerprint and is the most direct, easily obtained information. The best example of this is the series CH_4, C_2H_4, and C_2H_2 where the local carbon hybridization is sp^3, sp^2, and sp, respectively.[5] As can be seen from Figure 2, the CH_4 and C_2H_4 spectra are dramatically different, and the C_2H_2 spectrum[5] is different from either of these, while the normal alkanes[6] all share the same general spectral line shape as methane. With use of these fingerprints, the methyl cyanide C(KVV) spectrum can be approximated very well as a sum of a C_2H_2 spectrum used as a model for the cyanide group C and a CH_4 spectrum used to model the methyl group C.[8]

Also included in Figure 2 are spectra of ethylene, cyclopropane, and cyclohexane.[7] Despite formally having four bonds to each carbon as in the normal alkanes, the spectrum of cyclopropane is dramatically different from the general fingerprint of a tetrahedral sp^3-hybridized carbon atom[6] but can be seen to be nearly identical with the spectrum from the sp^2-hybridized carbon atom in ethylene.[7] This similarity between ethylene and cyclopropane, consistent with similarities observed in a comparison of their chemical behavior,[16] total electron density determinations,[17] and valence-orbital structure,[18] is due to the highly strained bond angles in cyclopropane. The spectral series for cyclopropane through cyclohexane[7] illustrates this point. As the bond angles systematically increase from cyclopropane through cyclohexane (only the end examples are shown in Figure 2), the character of the Auger spectra smoothly converts from ethylene-like to alkane-like. The spectrum for cyclohexane, where the molecule is large enough to have pure tetrahedral bond angles, is identical with that of normal hexane.

One can also see the same local fingerprint character in the C(KVV) spectra of the metal carbonyls shown

(15) J. A. D. Matthew and Y. Komninos, *Surf. Sci.*, **53**, 716 (1975).

(16) R. A. Raphael, "Chemistry of Carbon Compounds", E. H. Rodd, Ed., Elsevier, Amsterdam, 1953, p 23.

(17) G. L. Delker, Y. Wans, G. D. Stucky, R L. Lambert, Jr., C. K. Haas, and D. Seyforth, *J. Am. Chem. Soc.*, **98**, 1779 (1976).

(18) E. Lindholm, C. Fridh, and L. Asbrink, *Faraday Discuss. Chem. Soc.*, **54**, 127 (1972).

in the top portion of Figure 3. The spectra are plotted on a two-hole binding-energy scale obtained by subtracting from the Auger electron energies the value of the appropriate core-level binding energy. The use of such a two-hole energy scale, which contains only final-state valence terms (eq 1), assures that transitions from different atomic locations in the same molecule will occur at the same relative energy. Despite the major differences in molecular structure for these carbonyls, the local bonding structure of the carbonyl group is the same, and as a result they share the same local spectral fingerprint. These spectra and those for CO and NO will be discussed in more detail below.

Local Effects in Auger Transition Energies

Prime examples of localization, both in chemical bonding and Auger spectroscopy, are found in the normal alkanes.[6,20] Selected Auger spectra for this group of molecules is shown in Figure 2. The experimental core-binding energies for the alkanes are found to vary by only a few tenths of an electronvolt.[21] While the valence levels broaden into a band of states with increasing size, the splitting is uniform in energy about the value corresponding to the equivalent states of methane.[22,23] One-electron theory that involves delocalized MO's would predict a hole–hole repulsion for the alkanes that decreases with increasing molecular size.[6] As a result, a set of spectra that systematically shifts to higher kinetic energy with increasing size is expected.[6] The lack of such a shift for the principal structure in the spectra of Figure 2 (and with the alkanes in general through polyethylene[6,20]) shows that one-electron theory is not entirely adequate in this case. Moreover, the normal alkanes can be approximately characterized by a common value of U (obtained from eq 1) of magnitude consistent with Auger final-state localization to a single-carbon subunit.

Similar local effects are seen in the spectra of the metal carbonyls. Since different atoms (C, N, and O) with different core bonding energies are available in the carbonyls and nitrosyls, the local nature of the Auger process means that one can view the same valence-electron structure from different atomic locations. Figure 3 illustrates the C(KVV) and N(KVV) spectra for CO, NO, and three metal carbonyls.[19] Only a limited set of the possible spectral combinations are shown here and ref 19 should be consulted for a more complete treatment.

Consider first the N(KVV) and C(KVV) spectra of NO and CO. The spectra of CO have been studied in considerable detail,[24] but here we will consider only the highest energy, chemically important transitions. Peak a in the CO spectrum results from a transition in which one final-state valence hole is in the 5σ level and one is in the 1π level, while peak b has both final state holes in the 5σ level, the highest occupied molecular orbital (HOMO). The 5σ is basically a lone-pair orbital with atomic-like properties and the two final-state holes in the 5σ state would be spatially compressed compared to the more diffuse $5\sigma^{-1}\,1\pi^{-1}$ final state. This leads to a larger hole–hole repulsion U for the $5\sigma^{-2}$ state and a shift to higher apparent two hole binding energy.

For comparison to NO, the main points to consider[19] are that the equivalent electrons of NO are slightly more tightly bound and that the 2π level in NO contains one electron, while for CO it is empty. These differences are reflected in the spectral detail of Figure 3. The one major difference between NO and CO is a large new peak c at a binding energy of −39 eV in the case of NO due to occupation of the 2π level. The one-electron binding energies corresponding to the Auger transitions a and b in Figure 3 are closer together and more tightly bound in NO, and the 5σ level of NO has less lone-pair character. As a result, peaks marked a and b in the CO spectrum collapse together and move slightly lower in energy to the peak marked a,b in the NO spectrum. As one might expect from the similar size and electronic structure of CO and NO, their hole–hole repulsion values are comparable.

In general, the metal carbonyls yield the same CO-derived C(KVV) fingerprint spectrum, Figure 3.[19] The photoelectron binding energies for the metal carbonyl states equivalent to those of CO are closer together and less tightly bound. The consequence of this is that the peaks marked a and b collapse together and move to slightly lower binding energy to form the peak marked a,b in Figure 3. Most of the energy shift between the CO and the metal carbonyl spectra can be accounted for on the basis of the one-electron binding-energy differences. This, of course, requires that the C(KVV) Auger spectrum of both CO and the metal carbonyls be accounted for by comparable values of the hole–hole repulsion U and, therefore, that the two final-state holes be localized to the same spatial extent in both free and bound CO. Theoretical calculations[19,25] yield a value of ΔU that is 5 times the splitting W due to the interaction between adjacent carbonyl groups, which is clearly within the localization regime and consistent with the experimentally observed localization.

The fact that Auger localization implies a breakdown of one-electron theory can be viewed as a problem in Auger spectroscopy. However, the fact that the Auger final state is localized to a carbonyl functional group also implies that the spectroscopy is a probe of the electronic structure of that functional group, or that AES is a functional-group-sensitive spectroscopy.

Peak c in the metal carbonyl spectra arises from occupation of the normally empty 2π level of CO.[19] In the case of the metal carbonyls, however, this occupation is due both to the molecular ground state and charge flow in response to creation of the initial carbon core hole. Bonding in the carbonyls involves overlap between a filled metal $d\pi$ and the normally empty 2π of CO. This would place electron density at the carbon site observable in the C(KVV) Auger. However, the intensity of peak c is too great to be supported by ground-state charge transfer and in large part is due to a flow of screening charge from the metal through the $d\pi$–2π bond in response to the creation of the initial-

(19) G. D. Stucky, R. R. Rye, D. R. Jennison, and J. A. Kelber, *J. Am. Chem. Soc.*, **104**, 5951 (1982); D. R. Jennison, G. D. Stucky, R. R. Rye, and J. A. Kelber, *Phys. Rev. Lett.* **46**, 911 (1981).

(20) J. A. Kelber, R. R. Rye, G. C. Nelson, and J. E. Houston, *Surf. Sci.*, **116**, 148 (1982).

(21) J. J. Pireaux, R. Candano, S. Svensson, E. Basilier, P. A. Malmqvist, U. Gelius, and K. Siegbahn, *J. Phys. (Orsay, Fr.)*, **38**, 1213 (1977); **38**, 1221 (1977).

(22) J. N. Murrell and W. Schmidt, *J. Chem. Soc., Faraday Trans.*, **268**, 1709 (1972); A. D. Baker, D. Berreridge, N. R. Kemp, and R. E. Kirby, *J. Mol. Struct.*, **8**, 75 (1972).

(23) R. Hoffman, *J. Chem. Phys.*, **40**, 2047 (1963).

(24) J. A. Kelber, D. R. Jennison, and R. R. Rye, *J. Chem. Phys.*, **75**, 652 (1981).

(25) G. Loubriel, *Phys. Rev. B*, **20**, 5339 (1979).

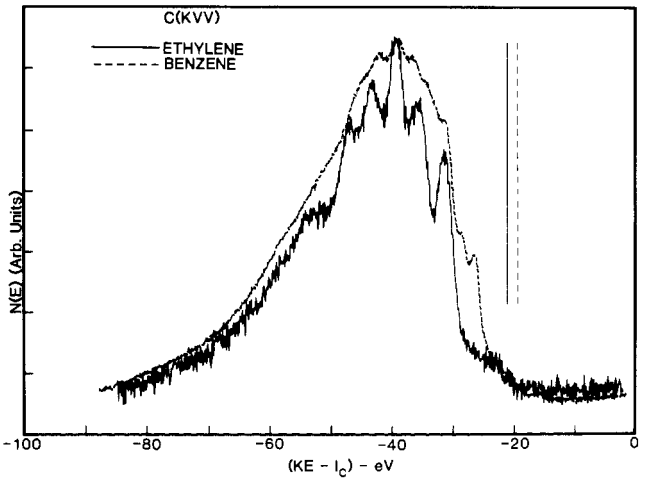

Figure 4. C(KVV) Auger spectra for benzene and ethylene plotted on a common two-hole energy scale obtained by subtracting the core bonding energies from the respective experimental Auger kinetic energies.

state core hole on the carbonyl carbon.

The examples considered to this point have been ones that are representative of localized chemical bonding, and the general result is that the Auger line shapes reflect this localization as indicated by the magnitude of U. In contrast, the classical example of delocalized chemical bonding is in the π-electron system of aromatic compounds. The C(KVV) Auger spectrum of benzene is shown in Figure 4, again plotted on a two-hole binding-energy scale. This line shape, though less well-resolved, is identical with that reported by Siegbahn et al.[3] For comparison, Figure 4 also contains the spectrum of ethylene.[5] For ethylene and benzene in Figure 4, as well as for naphthalene and biphenyl,[26] there is a general correspondence below ~35 eV in the spectral features. Line-shape differences in these four molecules are seen primarily in the region above ~35 eV as is clearly evident for the spectra structure in the comparison shown in Figure 4. The spectrum of biphenyl is identical, with reduced resolution, with the benzene results in Figure 4. The only difference with naphthalene is that the threshold is moved a few volts higher in energy.

This comparison between ethylene and the aromatic molecules is clearly suggestive of the bonding similarities and differences in the three molecules. Each can be viewed as containing a σ framework resulting from overlap between adjacent sp^2-hybridized carbon atoms and a π system resulting from overlap of the remaining carbon p electrons. The σ framework comprises the deeper lying one-electron energy levels and can be expected to correspond to the higher binding-energy region of the Auger spectrum in Figure 4, while the π orbitals are the higher lying states and correspond to the low binding energy portion of the spectrum. The σ framework formally results from the same type of bonding as that for the normal alkanes (the only difference being the hybridization of the carbon atom), and by analogy one would expect the Auger transitions involving these levels to be localized. The result would be, as we see in Figure 4, spectral contributions that occur at the same energy independent of the size difference between ethylene and benzene.

(26) R. R. Rye and J. E. Houston, unpublished results.

Thus, the σ framework is expected to show localized behavior in both a chemical and an Auger sense. The π system, however, is chemically delocalized. If this delocalized behavior held in the Auger case, then the implication would be that one would find a value of U that decreases with increasing extent of delocalization or physical size. In Figure 4 the vertical lines give the energy corresponding to twice the binding energy of the HOMO.[27] Given eq 1, the energy distance between the vertical line and the first feature in the experimental spectrum should be the hole–hole repulsion U for the Auger transition leading to two holes in the HOMO. Clearly this U is less for benzene (7.7 eV) then that found for ethylene (10.5 eV). Both should be compared to the 14 eV found for methane and the higher normal alkanes that have localized characteristics in both a chemical and an Auger sense. Assuming that U scales like $1/r$, i.e., that U is a Coulomb repulsion term, and that the 14-eV value in methane is due to delocalization at most to adjacent hydrogen atoms, one would predict a U of 10.5 eV for ethylene on the basis of the carbon–carbon bond distance and a value of 8.9 eV for benzene considering delocalization limited by the maximum carbon–carbon distance.

Local Effects in Auger Transition Intensities

As a result of the large differences in electron density existing in the same orbital at different atomic locations, highly polar materials are particularly good examples of the variation in the relative Auger intensity for transitions to the same final state from different atomic locations. In the case of the tetrahedral halides, moreover, the high degree of degeneracy in the molecular orbitals, resulting from the symmetry of the molecule, yields the ability to differentiate between energetically degenerate but spatially separate orbitals. Considering first the Auger intensity variation, this can be illustrated with the spectra for SiF_4 given in Figure 5.[28] The energy spacings of the bar graphs in Figure 5 were obtained from a self-fold on the one-electron binding energies[29] following eq 1 and assuming a constant value of U. The intensities for each of the transitions were obtained from eq 3 with use of published populations[30] and atomic matrix elements.[9]

The interpretation of the F(KVV) spectrum is relatively straightforward. The general shape of the spectrum is found to be very similar to that of neon. Furthermore, good agreement is obtained between the bar graph and the experimental spectrum for a U of 18.5 eV, a value only a few volts less than the experimental value for neon.

The interpretation of the Si(LVV) spectrum, however, is not straightforward despite the fact that there is a paucity of transitions in the Si spectrum compared to that of F. The arrows in Figure 5 serve to align transitions in the bar graphs that correspond to the same final-state hole combination. Basically the Auger intensity is proportional to the atomic-like electron density at the initial core-hole site. Clearly this is a maximum for lone-pair electrons. As a result the major

(27) J. W. Robinson, Ed., "Handbook of Spectroscopy", CRC Press, Cleveland, OH, 1974, Vol. 1.
(28) R. R. Rye and J. E. Houston, *J. Chem. Phys.*, 78, 4321 (1983).
(29) W. B. Perry and W. L. Jolly, *J. Electron Spectrosc. Relat. Phenom.*, 4, 219 (1974).
(30) A. E. Jonas, G. K. Schweitzer, F. A. Grimm, and T. A. Carlson, *J. Electron Spectrosc. Relat. Phenom.*, 1, 29 (1972).

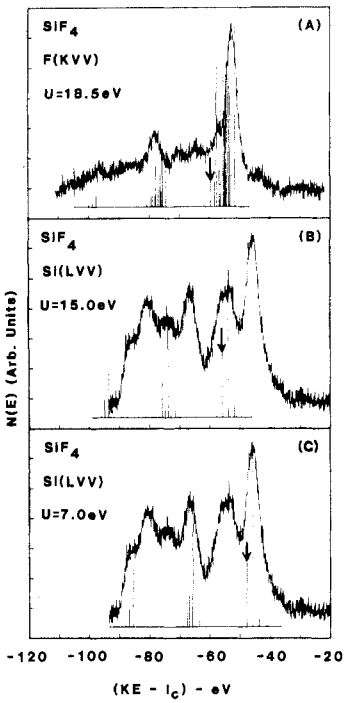

Figure 5. F(KVV) and Si(LVV) Auger spectra for SiF_4 plotted on a common two-hole energy scale obtained by subtracting the core binding energies from the respective experimental Auger kinetic energies. The bar graphs are obtained from a self-fold of the one-electron binding energies for the relative energy positions with the relative intensities calculated from the atomic orbital parentages of the molecular orbitals. The value of U in each case is the energy shift necessary to obtain the alignments shown.

peaks in the F(KVV) spectrum are lone-pair derived, while the transitions involving the Si–F bonding electrons are relatively weak, reflecting in part the delocalization of electron density to the bonding region. The converse, of course, is that the Si core hole has essentially zero overlap with the F lone pairs, which, as a result, do not contribute to the Si(LVV) spectrum. As a result of these intensity variations, the F spectrum is dominated by lone-pair contributions, while the bonding electrons are best seen in the Si(LVV) spectrum.

The experimental Si(LVV) spectrum of Figure 5 appears more complex than that expected from a one-electron model containing, as it does, six experimental structures compared to only three in the corresponding bar graph. As a matter of fact, the experimental spectrum appears to be composed of contributions from two bar graph like components displaced in energy by ~7 eV as illustrated in Figures 5B and 5C. We interpret this behavior to result from the highly polar and degenerate character of the bonding in SiF_4. For an Auger transition involving a given bonding orbital, the process will occur (eq 3) through that portion of the valence-electron density immediately around the Si-atom site. Because of the polar character of the bonding orbitals, however, the resulting final-state hole density will appear primarily around the F-atom site. Because of the energy degeneracy involved in SiF_4, the two final-state holes have the possibility of being on the same F site or on separate F sites. In a one-electron sense, with energetically degenerate orbitals, these two processes would be equivalent in energy, but for the Auger process one has to consider the hole–hole repulsion term in eq 1. For holes on separate sites (i.e., in energetically degenerate but spatially different orbitals), the hole separation would be larger and U smaller as in Figure 5C. For holes on the same site, the separation should be smaller and U larger as in Figure 5B. Thus in this case, AES differentiates between energetically degenerate states on the basis of their spatial characteristics.

Given this model one can obtain a good approximation to the U values for SiF_4 from molecular dimensions, under the assumption that U scales as $1/r$ (where r is the effective separation between holes) and with use of the experimental size and U value for Ne.[28] For characteristic values of r approximated by the fluoride ion radius for Figure 5A, the Si–F bond distance for Figure 5B and the F···F distance for Figure 5C, values of 17.0, 14.8, and 9.0 eV, respectively, are calculated. This same crude calculation has been compared to the experimental value of U for 17 specific molecular examples and have been found to be generally successful to within several electronvolts.[28]

The tetrahalide series also allows a straightforward interpretation in terms of molecular dimensions of the criterion for localization or delocalization in their Auger spectra. As mentioned earlier, for $\Delta U/W$ greater than 1, localization is expected, while a ratio less than 1 leads to a delocalized behavior. The effect of W and ΔU can be seen in the halide spectra for the series: SiF_4, CF_4, $SiCl_4$, and CCl_4.[28] For example, the F(KVV) spectra of SiF_4 and CF_4 are found to be very similar with the exception of a structure on the low binding energy side of the spectrum of CF_4, which is at most only weakly present in the SiF_4 result. This structure is due to a delocalized component in the spectrum, i.e., the result of a small interaction between the lone-pair orbitals on neighboring F's such that some probability exists for placing one of the final-state holes on one of the F neighbors. In going from SiF_4 to CF_4 the F···F distance has decreased due to the shorter C–F bond distance. This would lead to a greater F–F interaction (a larger W) and a smaller ΔU in the case of CF_4 and, as observed, a greater degree of delocalization in the spectrum. A molecular-level measure of this interaction would be the ratio of the halide–halide separation to the radius of the halide ion itself. This ratio is 1.9 for SiF_4 and 1.6 for CF_4. For $SiCl_4$ the ratio is back up to 1.8 and an argon-like Cl(LVV) spectrum is observed; for CCl_4 the ratio is 1.6, and here again, a significant delocalized component is observed on the low binding energy side of the Cl(LVV) spectrum.

Discussion and Conclusions

Due to the local character of the Auger process, Auger electron spectroscopy has been shown to yield a unique local view of valence-electronic structure. The information content can be divided into three broad classes: (1) local symmetry sensitivity contained in the overall spectral fingerprint, (2) an apparent ability to differentiate between localized and delocalized bonding systems on the basis of the hole–hole repulsion energy, and (3) a measure of the orbital density distributions contained in the relative transition intensity distributions from various atomic species within the molecule.

With respect to the Auger final state, the rules for determining the degree to which the final-state holes will be spatially localized are very similar to those used for describing local/delocal chemical bonding. The only

difference is that in the Auger case the important relative strengths involve the energy of the localized hole–hole interaction compared to the strength of the bonding interaction. As was discussed by Ramaker,[9] if the holes in a given bond or group of bonds interact strongly relative to the strength of the covalent interaction of this bond or group with the rest of the system, then the holes will tend to remain in the locality of the bond or group. The important point to note here is the fact that the hole–hole interaction in the Auger final state reflects the local/delocal properties of the chemical bonding (although the effect may be enhanced in the two-hole situation), and information concerning these properties are made available in the spectral line shape through the U term in eq 1.

The major theme throughout this Account has been on the local nature of AES as a valence spectroscopy. The ability to obtain direct valence information specific to atomic locations in a large matrix is clearly the attribute of AES that makes it interesting and applicable to a wide variety of chemical problems. Examples of the breadth of this applicability include the following: work in progress directed toward obtaining a better understanding of the adhesion characteristics of metal films on polymers,[20] characterization of active carbon species present on various metal surfaces during the methanation reaction,[31] obtainment of an understanding of the initiation sensitivity of aromatic explosives,[32] relation of the local/delocal nature of the d band in transition-metal alloys to their magnetic properties,[33] and studies of the chemical nature of chemisorbed species on metal substrates.[34] An equally interesting, but as yet untouched, area concerns applications of AES to biological systems, e.g., to studies of the chemical nature of the active metal sites in metal porphyrin based systems. At this point, the general applicability of AES is limited more by a lack of confidence resulting from the narrowness of past experience than by inherent difficulties with the technique itself.

The authors wish to acknowledge the contributions of J. W. Rogers, Jr., through many useful discussions and his careful reading of the manuscript.

(31) J. E. Houston, D. E. Peebles, and D. W. Goodman, *J. Vac. Sci. Technol.*, A1, 995 (1983).
(32) J. W. Rogers, R. R. Rye, and J. E. Houston, unpublished results.
(33) P. A. Bennett, J. C. Fuggle, and F. V. Hilledbrecht, *Phys. Rev. B*, in press.
(34) J. E. Fuggle, E. Umback, R. Kakoschke, and D. Menzel, *J. Electron Spectrosc. Relat. Phenom.*, **26**, 111 (1982).

Additions and Corrections

1983, Volume 16

R. M. Hochstrasser and H. P. Trommsdorf: Nonlinear Optical Spectroscopy of Molecular Systems.

Page 385. The following paragraph was inadvertently omitted:

The individuals from this laboratory who are cited in the text are responsible for bringing about the developments in nonlinear molecular spectroscopy that form the main thrust of this Account. The first nonlinear spectroscopy at The University of Pennsylvania was initiated by John E. Wessel, with extensions into coherent processes being made by G. R. Meredith, I. I. Abram, P. L. Decola, F. Ho, W.-S. Tsay, John Trout, H. Souma, E. J. Heilweil, R. Bozio, and B. Dick. The recent studies of fully resonant interactions were initiated by J. R. Andrews. We are deeply indebted to all of the aforementioned students, postdoctoral fellows, and visitors for their invaluable contributions to the research summarized in this Account.